THE JOURNAL OF BIOLOGICAL CHEMISTRY VOL. 289, NO. 45, pp. 31591–31604, November 7, 2014

Loss of Ypk1, the Yeast Homolog to the Human Serum- and Glucocorticoid-induced Protein Kinase, Accelerates Phospholipase B1-mediated Phosphatidylcholine Deacylation*

Received for publication, May 13, 2014, and in revised form, September 13, 2014 Published, JBC Papers in Press, September 25, 2014, DOI 10.1074/jbc.M114.581157

Beth A. Surlow[‡], Benjamin M. Cooley[‡], Patrick G. Needham[§], Jeffrey L. Brodsky[§], and Jana Patton-Vogt[‡1]

From the [‡]Department of Biological Sciences, Duquesne University, Pittsburgh, Pennsylvania 15282 and the [§]Department of Biological Sciences, University of Pittsburgh, Pittsburgh, Pennsylvania 15260

Background: Ypk1 is a protein kinase known to regulate sphingolipid homeostasis. Plb1 deacylates phosphatidylcholine to produce glycerophosphocholine.
Results: Loss of Ypk1 or disruption of sphingolipid synthesis by other means elevates Plb1-mediated phosphatidylcholine turnover.
Conclusion: Accelerated turnover of phosphatidylcholine compensates for aberrant sphingolipid synthesis.
Significance: Sphingolipid synthesis is coordinated with phosphatidylcholine metabolism to maintain membrane lipid homeostasis.

Ypk1, the yeast homolog of the human serum- and glucocorticoid-induced kinase (Sgk1), affects diverse cellular activities, including sphingolipid homeostasis. We now report that Ypk1 also impacts the turnover of the major phospholipid, phosphatidylcholine (PC). Pulse-chase radiolabeling reveals that a *ypk1*Δ mutant exhibits increased PC deacylation and glycerophosphocholine production compared with wild type yeast. Deletion of *PLB1*, a gene encoding a B-type phospholipase that hydrolyzes PC, in a *ypk1*Δ mutant curtails the increased PC deacylation. In contrast to previous data, we find that Plb1 resides in the ER and in the medium. Consistent with a link between Ypk1 and Plb1, the levels of both Plb1 protein and *PLB1* message are elevated in a *ypk1*Δ strain compared with wild type yeast. Furthermore, deletion of *PLB1* in a *ypk1*Δ mutant exacerbates phenotypes associated with loss of *YPK1*, including slowed growth and sensitivity to cell wall perturbation, suggesting that increased Plb1 activity buffers against the loss of Ypk1. Because Plb1 lacks a consensus phosphorylation site for Ypk1, we probed other processes under the control of Ypk1 that might be linked to PC turnover. Inhibition of sphingolipid biosynthesis by the drug myriocin or through utilization of a *lcb1-100* mutant results in increased *PLB1* expression. Furthermore, we discovered that the increase in *PLB1* expression observed upon inhibition of sphingolipid synthesis or loss of Ypk1 is under the control of the Crz1 transcription factor. Taken together, these results suggest a functional interaction between Ypk1 and Plb1 in which altered sphingolipid metabolism up-regulates *PLB1* expression via Crz1.

Ypk1, the yeast homolog of the human serum- and glucocorticoid-induced kinase (Sgk1), is a serine/threonine protein kinase known to affect multiple downstream processes, including lipid homeostasis (1–5), actin dynamics (6, 7), cell wall integrity (6, 7), endocytosis (3, 8), and lipid flippase activity (1). Ypk1 has a functionally redundant homolog, Ypk2 (Ykr2). Either Ypk1 or Ypk2 is required for cell viability, but Ypk1 plays a more prominent role in several processes (6, 9). For example, deletion of *YPK1* results in a growth defect and increased sensitivity to several drugs, phenotypes that are not observed in the *ypk2*Δ mutant (6). Ypk1, a cytosolic protein, is recruited to the plasma membrane through its interaction with Slm1/2, proteins that contain a pleckstrin homology domain that mediates binding to phosphatidylinositol 4,5-bisphosphate (10, 11). At the plasma membrane, Ypk1 is first activated by TORC2 (target of rapamycin complex 2) (10, 11) and then by Pkh1/2 phosphorylation (6). TORC2 has been shown to be activated by sphingolipid depletion (12) and elevated reactive oxygen species (13). In turn, Pkh1 and Pkh2, homologs of the PDK1 (mammalian phosphoinositide-dependent protein kinase 1) family, preferentially phosphorylate and activate Ypk1 and Ypk2, respectively, although some crossover is observed (6). Pkh1 and Ypk1 are localized exclusively to the cytosol, whereas Pkh2 and Ypk2 also enter the nucleus. Exogenous addition of the long chain base phytosphingosine activates Pkh1/Pkh2 *in vitro* as measured by an increase in PKC phosphorylation (14), whereas a more recent paper suggests that the ability of Pkh1/2 to activate Ypk1/2 is unaffected by long chain bases but instead requires the complex sphingolipid, mannosylinositol phosphorylceramide (1).

The known targets of Ypk1 phosphorylation, Fpk1/2 (1), Orm1/2 (2), and Gpd1 (15), are all involved in some aspect of lipid metabolism. Ypk1 phosphorylates and thereby inactivates Fpk1 and Fpk2, which are upstream activators of the lipid flippase complexes, Lem3-Dnf1 and Lem3-Dnf2, respectively (1,

* This work was supported, in whole or in part, by National Institutes of Health Grants R15 GM104876 (to J. P. V.) and R01 GM75061 and P30 DK79307 (to J. L. B.). The purchase of mass spectrometers was supported by National Science Foundation Grant MRIDBI-0821401.
[1] To whom correspondence should be addressed. Tel.: 412-396-1053; Fax: 412-396-5907; E-mail: pattonvogt@duq.edu.

TABLE 1
***S. cerevisiae* strains used in this study**

Strain		Genotype	Reference or source
JPV 399	WT, BY4742	BY4742; *MATα his3Δ1 leu2Δ0 lys2Δ0 ura3Δ0*	Research Genetics
JPV 636	*ypk1Δ*	BY4742; *ypk1Δ::KanMX*	Research Genetics
JPV 668	*plb1Δ*	BY4742; *plb1Δ::hph*	This study
JPV 766	*ypk1Δplb1Δ*	BY4742; *ypk1Δ::KanMX plb1Δ::hph*	This study
JPV 744	WT *PLB1-I-3xHA*	BY4742; *PLB1-I-3xHA*	This study
JPV 745	*ypk1Δ PLB1-I-3xHA*	BY4742; *ypk1::KanMX PLB1-I-3xHA*	This study
JPV 671	*crz1Δ*	BY4742; *crz1Δ::KanMX*	Research Genetics
JPV 782	*crz1Δypk1Δ*	BY4742; *crz1Δ::KanMX ypk1Δ::URA3*	This study
JPV 680	*plb123Δnte1Δ*	BY4742; *plb1Δ::hph plb2Δ::KanMX plb3Δ::nat nte1Δ::ble*	This study
JPV 706	*fpk1Δ*	BY4742; *fpk1Δ::KanMX*	Research Genetics
YPH 499	WT, YPH499	*MATa ade2-101^{och} his3Δ200 leu2Δ1 lys2-801^{am} trp1Δ1 ura3-52*	Ref. 6
YES 3	*ypk1Δ*	YPH499; *ypk1-Δ1::HIS3*	Ref. 6
YES 1	*ypk2Δ*	YPH499; *ypk2-Δ1::TRP1*	Ref. 6
YPT 40	*ypk1^{ts}ypk2Δ*	YPH499; *ypk1-1^{ts}::HIS3 ypk2-Δ1::TRP1*	Ref. 6
JPV 772	*plb1Δ*	YPH499; *plb1Δ::hph*	This study
JPV 773	*ypk1Δplb1Δ*	YPH499; *ypk1-Δ1::HIS3 plb1Δ::hph*	This study
JPV 774	*ypk1^{ts}ypk2Δplb1Δ*	YPH499; *ypk1-1ts::HIS3 ypk2-Δ1::TRP1 plb1Δ::hph*	This study
RH 406	WT	*MATα leu2 trp1 ura3 bar1*	Ref. 71
RH 3804	*lcb1-100*	*MATα leu2 trp1 ura3 bar1 lcb1-100^{ts}*	Ref. 71
DDY 904	WT, DDY904	*MATa his3-Δ200 leu2-3, 112 ura3-52*	Ref. 36
DDY 5117	*orm1Δorm2Δ*	DDY904; *orm1Δ::CgLEU2 orm2Δ::CgURA3*	Ref. 36
DDY 5118	*orm1Δorm2^{Asp}*	DDY904; *orm1Δ::CgLEU2 3XFLAG-orm2 (S46D, S47D, S48D)::NAT*	Ref. 36
DDY 5119	*orm1Δorm2^{Ala}*	DDY904; *orm1Δ::CgLEU2 3XFLAG-orm2 (S46A, S47A, S48A)::NAT*	Ref. 36
JPV 807	*ypk1Δ*	DDY904; *ypk1Δ::hph*	This study
JPV 808	*orm1Δorm2Δ ypk1Δ*	DDY904; *orm1Δ::CgLEU2 orm2Δ::CgURA3 ypk1Δ::hph*	This study
JPV 810	*orm1Δorm2^{Asp} ypk1Δ*	DDY904; *orm1Δ::CgLEU2 3XFLAG-orm2 (S46D, S47D, S48D)::NAT ypk1Δ::hph*	This study

16). Ypk1 phosphorylation of the endoplasmic reticulum (ER)[2] transmembrane proteins, Orm1 and Orm2, renders them unable to bind to and inhibit serine palmitoyltransferase (SPT), the rate-limiting step in sphingolipid biosynthesis (2, 17, 18). Finally, Ypk1 phosphorylates and inactivates Gpd1 (glycerol-3-phosphate dehydrogenase), which reduces dihydroxyacetone phosphate (15). The product of this reaction, glycerol 3-phosphate, can be shuttled into multiple metabolic pathways, including phospholipid biosynthesis.

Another finding linking Ypk1 to lipid metabolism is that overexpression of the B-type phospholipase, *PLB1*, rescues the lethality of the temperature-sensitive *ypk1^{ts} ypk2*Δ mutant (1). The B-type phospholipases (PLBs) catalyze the deacylation of glycerophospholipids to produce the glycerophosphodiesters and free fatty acids (Fig. 1*A*). In *Saccharomyces cerevisiae*, four genes encode proteins with PLB activity, *PLB1*, *PLB2*, *PLB3*, and *NTE1*, which function in membrane remodeling in the cell. Based on *in vivo* studies, Plb1 primarily deacylates phosphatidylcholine (PC) to produce external glycerophosphocholine (GroPCho) (19). Biochemical studies have suggested that Plb1 is plasma membrane-associated and secreted from the cell (19–21), whereas Nte1 is localized to the ER and is responsible for the production of internal GroPCho (22). The primary substrate for Plb2 appears to be exogenous phospholipids, and Plb3 acts on phosphatidylinositol (PI) to produce extracellular glycerophosphoinositol (20, 21).

PC synthesis and catabolism are tightly regulated in yeast (23) and other eukaryotic cells (24), and disruptions to PC metabolism can result in aberrant physiological responses. In mammalian cells, increased choline uptake and incorporation into PC is a marker for proliferative growth (25), and conversely, inhibition of choline synthesis results in apoptosis (26). Aberrant PC levels and/or alterations in GroPCho have also been observed in patients with various cancers, such as colorectal (27) and prostate (28) cancer, and in Alzheimer disease (29, 30). What has remained unknown, however, is how protein kinases and members of the B-type phospholipases, which deacylate phospholipids to produce GroPCho, are coordinately regulated to ensure lipid homeostasis. Here, we describe a novel role for Ypk1, the yeast homolog of Sgk1, in regulating Plb1-mediated PC turnover.

EXPERIMENTAL PROCEDURES

Strains, Plasmids, Media, and Growth Conditions—The *S. cerevisiae* strains used in this study are shown in Table 1. Strains were grown aerobically with shaking at 30 or 37 °C, as noted. Turbidity was monitored by measuring the optical density at 600 nm (A_{600}) on a BioMate 3 Thermo Spectronic spectrophotometer. Empty vectors, YEp351 and pRS426, and vectors overexpressing each of the PLB genes, YEp351-*PLB1*, YEp351-*PLB2*, YEp351-*PLB3*, and pRS426-*NTE1*, were gifts from Susan Henry (YEp351 series) (21) and Chris McMaster (pRS426-*NTE1*) (31). Media used for this study included rich yeast extract peptone dextrose (YPD) medium purchased from Fisher or synthetic complete yeast nitrogen base (YNB) medium containing amino acids, 2% glucose, and 75 μM inositol, as described previously (32).

Construction of Strains—The *S. cerevisiae* WT strain BY4742 was purchased from Open Biosystems (Thermo Scientific, Huntsville, AL). The deletion strains were constructed using standard homologous recombination techniques (33). Drug-resistant markers, *hphMX*, *KanMX*, *natMX*, and *ble*, were amplified from plasmids pAG32, pUG6, pAG25, and pUG66, respectively, using the primers listed in Table 2, and the resulting DNA fragments were inserted in place of the genes targeted for deletion. The plasmids were received from Euroscarf (34,

[2] The abbreviations used are: ER, endoplasmic reticulum; PC, phosphatidylcholine; GroPCho, glycerophosphocholine; PLB, B-type phospholipase; PI, phosphatidylinositol; YNB, yeast nitrogen base; TLC, thin layer chromatography; SPT, serine palmitoyltransferase; YPD, yeast extract peptone dextrose; GPI, glycosylphosphatidylinositol; BisTris, 2-[bis(2-hydroxyethyl)-amino]-2-(hydroxymethyl)propane-1,3-diol.

TABLE 2
Nucleotide sequences of primers used for gene deletions
The deleted gene was replaced with the gene name in parentheses. Boldface sequences are homologous to the template plasmids.

Gene name	Primer	Sequence (5′–3′)
PLB1 (*hph*)	Forward	CAAAACCATGAAGTTGCAGAGTTTGTTGGTTTCTGCTGCAGTTTTGACTTCTCTAAC**CAGCTGAAGCTTCGTACGC**
PLB1 (*hph*)	Reverse	AGAGCCTAAATTAGACCGAAGACGGCACTAATGACACTTAAGACACCA ATAAAAG**GCATAGGCCACTAGTGGATCTG**
YPK1 (*URA3*)	Forward	AGTTCCTCTCATATCAACAAACATTAATACAGTTCCTGAAAATGTATTCTTGGAAGTCAA**AGCGAACAAAAGCTGG**
YPK1 (*URA3*)	Reverse	ATGTATTCACTAAGTCTATCTAATGCTTCTACCTTGCACCATTGAGCTACCTAGCTGTTC**CTGTAGGGCGAATTGGG**
PLB1-I-3xHA	Forward	CTAACAGAGAACGTTAACGCTTGGTCACCAAATAACAGTTACGTC**AGGGAACAAAAGCTGG**
PLB1-I-3xHA	Reverse	TTCTCTGACTAAGTTAATATCATCATCACAGGTTACGTTCGCAGG**CTGTAGGGCGAATTGGG**
YPK1 (*hph*)	Forward	AGTTCCTCTCATATCAACAAACATTAATACAGTTCCTGAAAATGTATTCTTGGAAGTCAA**CAGCTGAAGCTTCGTACGC**
YPK1 (*hph*)	Reverse	ATGTATTCACTAAGTCTATCTAATGCTTCTACCTTGCACCATTGAGCTACCTAGCTGTTC**GCATAGGCCACTAGTGGATCTG**

35). *PLB1* was disrupted by insertion of *hphMX* in the YPH499 background strains provided by J. Thorner (6). *YPK1* was disrupted by insertion of *hphMX* in the *ORM* mutants and *ORM* phosphomimetic strains provided by D. Drubin (36). The N-terminal 3xFLAG-tagged *ORM2* allele was previously shown to be fully functional (36). For deletion of *YPK1* in the *crz1*Δ strain, the *URA3* cassette was amplified from plasmid pPMY-3xHA (37), and the resulting DNA fragment was used to disrupt *YPK1*.

[^{14}C]Choline Labeling and Preparation of External, Internal, and Membrane Fractions—Cells were grown to uniform labeling in synthetic medium containing 20 μM choline and 1 μCi/ml [^{14}C]choline chloride of negligible concentration (NEC141VU250UC (PerkinElmer Life Sciences) or ARC 0208 (American Radiolabeled Chemicals)). Cells were harvested in log phase, washed free of excess label, and reinoculated at A_{600} = 0.2 into synthetic medium containing 10 mM nonradioactive choline. At various time points, 1-ml aliquots of the chase cultures were removed and separated into external, internal, and membrane fractions (32, 38). In brief, cells were pelleted by centrifugation, and the supernatant was removed and retained as the extracellular fraction. The cell pellet was resuspended in 0.5 ml of 5% trichloroacetic acid (TCA), followed by a 20-min incubation on ice. Cells were pelleted again by centrifugation, and the supernatant was removed as the intracellular (soluble) fraction. The pellet was then resuspended in 0.5 ml of 1 M Tris (pH 8) and centrifuged, and the supernatant was added to the intracellular fraction. The final cell pellet was resuspended in 0.5 ml of 1 M Tris (pH 8) and saved as the membrane fraction. Total counts (external + internal + membrane) recovered at each time point as well as the percentages of counts in each fraction were tracked by liquid scintillation counting.

Analysis of Choline-containing Metabolites—The water-soluble choline-containing metabolites were separated by anion exchange chromatography (39). Internal and external samples were diluted 5-fold in deionized H_2O, applied to a 250-μl Dowex 50Wx8 200-400 anion exchange column, and eluted as described previously (39). [^{14}C]GroPCho was eluted with a 1-ml and 2-ml H_2O wash. If present, [^{14}C]choline phosphate was eluted with a subsequent 3-ml H_2O wash. [^{14}C]choline was eluted with 5 ml of HCl. Standards were used to verify the separation procedure, and label incorporated into each metabolite was quantified by liquid scintillation counting. To confirm results by independent methods, [^{14}C]choline-containing metabolites from selected samples were separated by TLC using previously published methods (40) and/or by HPLC with an in-line radioactive detector (41, 42). For TLC, samples were dried down, resuspended in 1:1 methanol/H_2O, and spotted on silica plates, and metabolites were separated with a mobile phase of CH_3OH, 0.6% NaCl, NH_4OH (50:50:5, v/v/v).

Phospholipids from the membrane fraction were extracted as described previously (43). The membrane pellet was resuspended in 1 ml of ESOAK (95% ethanol, diethylether, H_2O, pyridine, NH_4OH; 15:5:15:1:0.036) and incubated at 60 °C for 1 h. The suspension was centrifuged, and the lipid-containing supernatant was extracted with 2.5 ml of chloroform/methanol (2:1). Low speed centrifugation separated the layers, the bottom layer containing the glycerophospholipids was dried under N_2, and the residue was resuspended in chloroform/methanol (2:1). Radiolabeled PC and lyso-PC were resolved by TLC on Silica Gel 60A (Whatman) plates in chloroform, ethanol, H_2O, triethylamine (30:35:7:35, v/v/v/v) mobile phase (38, 44).

Analysis of Short Term Incorporation of [^{14}C]Choline into PC—Strains were grown to log phase (A_{600} = 0.5) in synthetic 75 μM inositol medium, harvested by centrifugation, and concentrated to equivalent densities in fresh synthetic medium containing 75 μM inositol and 100 μM choline. To start the assay, 50 μl of 0.005 mCi/ml [^{14}C]choline chloride was added, and cells were allowed to incubate for 30 min at 37 °C. The cells were pelleted by centrifugation, washed with water, and suspended in 0.5 ml of 5% TCA for 10 min. After pelleting, the supernatant was discarded, and the membrane pellet was washed with water. Lipids were extracted from the remaining pellet as described above. Incorporation of [^{14}C]choline chloride into PC was quantified by liquid scintillation counting and verified by TLC.

LC-MS Analysis of Extracellular Choline and GroPCho—Cells were grown in synthetic medium containing 75 μM inositol, 20 μM choline, and 2 mM KH_2PO_4 instead of 7 mM KH_2PO_4. The cells were pelleted by centrifugation at 1,600 × *g* for 3 min, and the supernatant containing the extracellular metabolites was filtered through 0.2-μm cellulose acetate filters. The method of analysis for these extracellular metabolites by mass spectrometry was described previously (45, 46). A 250-μl aliquot of supernatant was added to an internal standard (choline-d_9), and water-soluble lipid metabolites were extracted by the addition of 2.25 ml of chloroform/methanol (2:1, v/v). The suspension was agitated with a Vortex mixer followed by centrifugation for 3 min at 1,600 × *g*. The upper aqueous phase was dried under N_2 and resuspended in 125 μl of acetonitrile/methanol (75:25, v/v) with 10 mM ammonium acetate, pH 4.5. After centrifugation at 16,000 × *g* for 10 min, an aliquot of the supernatant was transferred to an LC vial and diluted 20-fold in acetonitrile/methanol (75:25, v/v). A 10-μl volume was injected

TABLE 3
Nucleotide sequences of primers used for qRT-PCR

Gene name	Primer	Sequence (5′–3′)
SNR17	Forward	TTG ACT CTT CAA AAG AGC CAC TGA
SNR17	Reverse	CGG TTT CTC ACT CTG GGG TAC
PLB1	Forward	GCA TAC ACC AAG GAG GCT TTG
PLB1	Reverse	GAG TGG ATA GCA AGG AAG TGT CAC

into the Agilent 1200 series Rapid Resolution LC system coupled to an Agilent 6440 triple quadrupole mass spectrometer. Separations were performed on a Waters Xbridge HILIC (150 × 4.6 mm, 5 μm) column with an isocratic elution at a flow rate of 0.5 ml/min at room temperature. The mobile phase was acetonitrile/water (70:30, v/v) with 10 mM ammonium acetate. Electrospray ionization MS was performed with the scan mode set to multiple reaction monitoring targeting GroPCho (258.0 → 104.0), choline (104.1 → 60.1), and choline-d_9 (113.1 → 69.1) in fast switch ionization mode. The MS parameters were set as previously optimized: collision energy, 10 eV; capillary voltage, 3.5 kV; fragmentor voltage, 50 V; dwell time, 200 ms; drying gas temperature, 300 °C; and sheath gas temperature, 325 °C. Sheath gas flow and drying gas flow rates were 10 and 8 liters/min, respectively. Each sample was run in duplicate. Data were acquired and analyzed using MassHunter Work Station software. The peak areas of the target metabolites were normalized to the internal standard and to the density of cells (A_{600}) from which metabolites were extracted.

RNA Extraction and Real-time Quantitative RT-PCR (qRT-PCR) Gene Expression Analysis—Cultures were grown in synthetic medium containing 75 μM inositol under the conditions specified. RNA was extracted using a hot phenol-chloroform extraction (47). A 7-μg sample of RNA was DNase-treated with 2 units of DNase at 37 °C for 30 min using the TURBO DNA-free™ kit (Applied Biosystems) per the manufacturer's specifications. Message abundance was quantified by qRT-PCR using the Verso™ SYBR® Green 1-Step QRT-PCR ROX kit (Thermo Scientific) on the Applied Biosystems StepOnePlus™ real-time PCR system. The primers used are shown in Table 3. Standard curves for each primer pair were optimized to determine acceptable primer concentrations (70–100 nM) and template concentrations (15–25 ng/25-μl reaction). Reverse transcription was carried out at 50 °C for 15 min, followed by 95 °C for 15 min for RT inactivation and polymerase activation. Amplification parameters were as follows: 40 cycles at 95 °C for 15 s, 54.5 °C for 30 s, and 72 °C for 40 s. Primer specificity was verified by melt curve analysis and visualization of amplicons by gel electrophoresis. Primer sets did not produce amplicons when RNA from the respective deletion strains was used as template. Control reactions without template and without reverse transcriptase were performed to verify the absence of genomic DNA contamination in the RNA samples and/or the reagents. RNA from at least three independent cultures of all strains was analyzed in triplicate reactions per primer set. Data were normalized to the endogenous control gene, *SNR17*, and analyzed using the comparative $\Delta\Delta C_T$ approach (48, 49).

Construction of the Chromosomal PLB1-I-3xHA Allele—The plasmid pPMY-3xHA (37), kindly provided by Nancy Hollingsworth (Stony Brook University), was used as the template to amplify a *3xHA-URA3* module for insertion into the genome between amino acids 30 and 31 of Plb1. Because Plb1 is predicted to be GPI-anchored to the plasma membrane, insertion at this point would avoid cleavage of the HA tag from either end because both the N-terminal localization signal and C-terminal GPI anchor attachment site are cleaved during processing and GPI anchor attachment. Insertion did not interfere with the predicted catalytic site for Plb1. The primers used to amplify the *3xHA-URA3* module are listed in Table 2. The PCR product was transformed into WT and *ypk1*Δ strains, and transformants were selected on synthetic plates lacking uracil. To verify integration at the correct location, DNA was extracted and used as template with two sets of primers. Verified transformants were grown in YPD liquid medium to allow for recombination and loss of the *URA3* marker. Cells that had lost the *URA3* marker were selected on synthetic plates containing 5-fluoroorotic acid. DNA was extracted from the 5-fluoroorotic acid-resistant colonies and used as a template for PCR. Strains producing the expected amplicon size, indicating insertion of the *3xHA* and loss of the *URA3*, were named JPV767 (WT + *PLB1-I-3xHA*) and JPV 745 (*ypk1*Δ + *PLB1-I-3xHA*). These strains therefore contain an internal *3xHA* tag between nucleotides 90 and 91 of *PLB1* in their genomic DNA. The function of Plb1 containing the *3xHA* tag was verified by observing the expected Plb1 activity in PC turnover/GroPCho production experiments.

Protein Extraction and Sucrose Gradient Separation—For total protein extraction from cell lysates, cultures were grown in synthetic + 75 μM inositol medium to log phase ($A_{600} \approx 0.7$). Cells were collected by centrifugation of a 125-ml culture, and the supernatant was removed for evaluation of secreted protein. The supernatant was concentrated 100-fold using an Amicon Ultra 30K centrifugal filter (Millipore). The cell pellet was resuspended in 200 μl of SUME protein lysis buffer (1% SDS, 8 M urea, 10 mM MOPS, 10 mM EDTA, 1 mM 4-benzenesulfonyl fluoride hydrochloride, 1× Yeast/Fungal Protease Arrest™ mixture (G-Biosciences catalog no. 786-333)) and lysed with glass beads by eight 1-min alternate cycles of agitation on a Vortex mixer and incubation on ice. Centrifugation at 2,000 × *g* for 5 min removed unbroken cells and debris. Protein concentration in the concentrated supernatant and the cell lysate was determined by a Bradford assay kit (Thermo Fisher).

Sucrose gradient separation was performed as described (50, 51). A 100-ml culture was grown to log phase, and 2 ml of 0.5 M NaN_3 was added at the time of harvest. The cells were collected by centrifugation and broken by glass bead lysis in a 10 mM Tris-HCl, pH 7.5, 1 mM EDTA, 10% sucrose solution. Cell lysates were cleared of debris by low speed centrifugation, and the resulting lysate was layered onto an 11-ml gradient of 30–70% sucrose in the lysis buffer. The gradient was centrifuged at 100,000 × *g* in a Beckman SW41 rotor for 18 h at 4 °C. 1-ml fractions were collected from the top of the gradient by pipetting. Proteins of interest were analyzed by SDS-PAGE and Western blot analysis.

Western Blot Analysis—Total protein extracts were analyzed by SDS-PAGE and Western blotting. An equal amount of protein was loaded onto NuPAGE BisTris gels (Invitrogen, IM-8042) and transferred to a nitrocellulose membrane using the XCell Blot Module (Invitrogen). Membranes were incu-

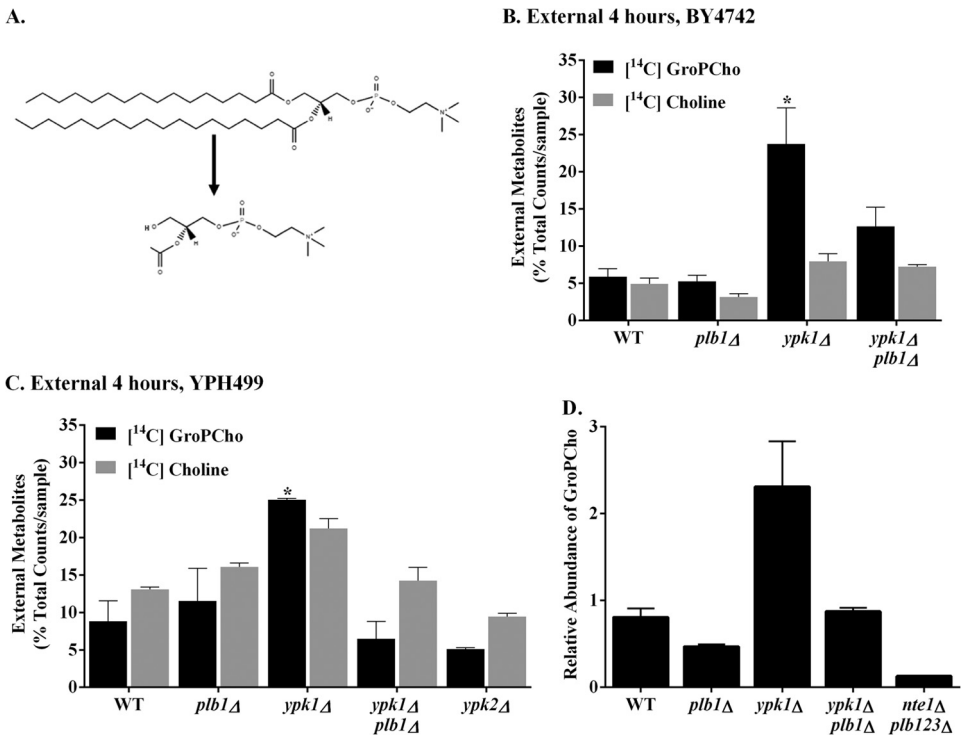

FIGURE 1. **Plb1-mediated extracellular GroPCho production is increased upon deletion of *YPK1*.** *A*, Plb1-mediated deacylation of PC to GroPCho. *B* and *C*, strains in the BY4742 (*B*) and YPH499 (*C*) backgrounds were pregrown at 30 °C in synthetic medium containing 0.2 μCi/ml [^{14}C]choline chloride, followed by a chase at 37 °C in synthetic medium containing 10 mM choline. Extracellular, intracellular, and membrane fractions were isolated, and [^{14}C]choline-containing metabolites from extracellular fractions were separated by anion exchange column chromatography. Values are the means ± S.E. (*error bars*) of triplicate cultures and are representative of multiple experiments. One-way analysis of variance was performed, indicating a significant difference between GroPCho produced in the *ypk1*Δ strain and GroPCho produced by each of the other strains listed (*A*, $p \leq 0.011$; *B*, $p \leq 0.015$). *D*, cells grown to log phase were harvested, and the extracellular medium was analyzed for GroPCho by LC-MS. Relative abundance is normalized to A_{600} and to the internal standard. Values are the means ± S.E. of at least two independent cultures.

bated in blocking buffer (phosphate-buffered saline (PBS) containing 5% casein in 0.1 M NaOH, 5% BSA, phenol red, and NaN_3) for 30 min at room temperature. Primary antibody against HA-Plb1 (monoclonal antibody HA-11, Covance catalogue no. MMS-101P) was added to the solution at a 1:10,000 dilution and incubated overnight at 4 °C. Primary antibody was removed, and the membrane was washed in PBS. The membrane was incubated in blocking buffer, without NaN_3, containing a 1:125,000 dilution of secondary antibody (HRP-labeled affinity-purified antibody to mouse IgG (H+L), KPL catalogue no. 074-1806) for 1 h at room temperature. The membrane was washed in PBS and incubated with SuperSignal West Femto extended duration substrate reagent (Pierce, catalog no. 34095) before exposure on either an Eastman Kodak Co. 440CF Image Station or exposure to Kodak Biomax MR film for visualization.

Sucrose gradient fractions were analyzed by SDS-PAGE and Western blot analysis as described for total protein extracts, but equal volumes of each fraction were run on the SDS-polyacrylamide gel instead of equal amounts of protein. Membranes were probed with primary antibodies against HA-Plb1, Sec61 (1:1,000), and Pma1 (1:4,000). Anti-Pma1 was provided by Dr. Carolyn Slayman (Yale University), and anti-Sec61 was obtained as described (52). The blots were then incubated with the appropriate secondary antibody, HRP-conjugated anti-rabbit or HRP-conjugated anti-mouse. For quantification of Western blots, densitometry was carried out using Kodak 1D software.

Statistical Analysis—GraphPad Prism was used for statistical analysis by Student's *t* test or analysis of variance as indicated.

RESULTS

Plb1-mediated Extracellular GroPCho Production Increases upon Loss of YPK1—Plb1 deacylates phosphatidylcholine to produce free fatty acids and extracellular GroPCho (19) (Fig. 1*A*). To better define the link between Ypk1 and Plb1 activity, turnover of PC and the concomitant production of the GroPCho were examined. Cells grown to uniform labeling with [^{14}C]choline chloride were washed free of label and reinoculated into fresh medium containing 10 mM choline at 37 °C. The chase was performed at elevated temperature to maximize turnover, because the Ypk1 pathway is activated by heat stress (1, 53) and because *PLB1* expression is up-regulated by elevated temperature (see Fig. 4*A*). These experiments were performed in both the BY4742 and YPH499 backgrounds because of slight differences in phenotypes observed in *ypk1*Δ *plb1*Δ double mutants constructed in the two backgrounds, as described below. At the indicated times, cells were harvested, the percentages of the total radioactivity in the extracellular, intracellular, and membrane fractions were determined, and the metabolites produced were identified. Radioactivity in the extracellular fraction, which is used to monitor *in vivo* Plb1 activity, consisted of [^{14}C]GroPCho and free [^{14}C]choline. As shown in Fig. 1, *B* and *C*, deletion of *YPK1* resulted in increased production of extracellular GroPCho that is ameliorated by deletion of *PLB1*.

TABLE 4
Values for the internal and membrane metabolites are derived from the experiment described in Fig. 1, *A* and *B*

Strain	Time	Cell-associated counts (percentage of total counts)			Total counts
		Internal Choline	Internal GroPCho	Membrane PC	
	h		%		
In BY4742					
WT	0	2 ± 0	34 ± 1	58 ± 3	94
	4	2 ± 0	81 ± 1	10 ± 0	93
*plb1*Δ	0	1 ± 0	38 ± 1	61 ± 3	99
	4	1 ± 0	76 ± 1	15 ± 1	92
*ypk1*Δ	0	1 ± 0	31 ± 1	66 ± 3	98
	4	1 ± 0	50 ± 4	18 ± 2	69
*ypk1*Δ *plb1*Δ	0	1 ± 0	35 ± 3	57 ± 4	92
	4	1 ± 0	55 ± 3	24 ± 1	80
In YPH499B					
WT	0	0 ± 0.2	7 ± 1	90 ± 1	97
	4	2 ± 0.4	14 ± 2	62 ± 2	82
*plb1*Δ	0	2 ± 1	13 ± 1	82 ± 1	97
	4	1 ± 0.1	9 ± 4	63 ± 1	82
*ypk1*Δ	0	2 ± 1	11 ± 1	84 ± 1	97
	4	2 ± 0.2	10 ± 2	53 ± 7	69
*ypk1*Δ *plb1*Δ	0	3 ± 1	15 ± 2	80 ± 3	98
	4	3 ± 0.5	8 ± 2	68 ± 3	70

This held true for both strain backgrounds, although the magnitude of the change varied from nearly 3-fold for YPH499 to roughly 5-fold for BY4742. The rest of the counts at each time point were in either the membrane or the intracellular fraction (Table 4).

Examination of the intracellular fractions revealed that there is a decrease in internal GroPCho production in both the *ypk1*Δ and the *ypk1*Δ*plb1*Δ strains (Table 4). Internal GroPCho production occurs primarily through Nte1-associated turnover (22), suggesting that there may be a trade-off between Nte1 and Plb1 activity upon loss of Ypk1. Loss of Ypk1 also appears to cause increased extracellular choline. The phospholipase D that hydrolyzes PC into free choline and phosphatidic acid (54), Spo14, could be responsible for the increase. Although quantitative differences in the levels of choline metabolites were observed as a function of strain background, the general trends were consistent. Also, deletion of *YPK2*, the paralog of *YPK1*, did not affect GroPCho production (Fig. 1*B*).

To confirm the results obtained through radiolabeling and to obtain a more complete picture of the extracellular choline metabolites produced, we performed tandem MS. Through radiolabeling, we were able to monitor the turnover of Kennedy pathway-derived PC synthesized during the labeling period. Through MS, we could monitor all GroPCho produced during the experiment through both the PE methylation pathway and through the Kennedy pathway (23). Importantly, the MS data confirmed that GroPCho production rose upon deletion of *YPK1* and that Plb1 plays a major role in facilitating the increase (Fig. 1*D*). Using MS, we also detected a decrease in extracellular GroPCho production by *plb1*Δ yeast as compared with wild type (WT) cells that was not apparent through pulse-chase radiolabeling. As indicated by both the MS data and the radiolabeling data, Plb1 cannot be the only phospholipase responsible for extracellular GroPCho production, because strains lacking Plb1 still produce GroPCho. In fact, a strain in which all of the known PLBs are deleted, *plb1,2,*3Δ*nte1*Δ, exhibits greatly reduced but not completely eliminated GroPCho production (Fig. 1*D*), suggesting that one or more deacylating phospholipases have yet to be identified.

Turnover of Another Glycerophospholipid, Phosphatidylinositol, Is Unaffected by Deletion of YPK1—In a WT strain, glycerophosphoinositol produced through the Plb3-mediated deacylation of PI is the major phospholipid metabolite found in growth medium (21). To monitor this metabolite, WT and *ypk1*Δ cells grown to uniform labeling with [^{3}H]inositol were chased with non-radiolabeled inositol, similar to the conditions used in the [^{14}C]choline labeling experiments above. However, we observed no significant difference between WT and *ypk1*Δ strains in the rate of PI turnover or in the percentage of water-soluble inositol-containing counts found in extracellular (WT, 31% ± 1; *ypk1*Δ, 25% ± 2) or intracellular (WT, 22% ± 1; *ypk1*Δ, 26% ± 3) fractions following a 5-h chase.

The Rate of Short Term Incorporation of [^{14}C]Choline into PC Is Unaffected by Loss of YPK1—Because an increased rate of PC deacylation and GroPCho production was observed upon loss of Ypk1, we next tested if the rate of incorporation of label into PC was affected. The logic underlying this experiment was that Cki1 (choline kinase) and Pct1 (choline phosphate cytidylyltransferase), both of which are involved in PC synthesis by the Kennedy pathway, contain potential consensus Ypk1 phosphorylation sites (R*X*R*XX*(S/T)ϕ, where ϕ is a preference for hydrophobic amino acids (9)). To detect changes in the synthesis rate via the Kennedy pathway, we measured the incorporation of [C^{14}]choline into PC following a 30-min pulse, which is short enough to result in minimal lipid turnover. No difference was found between WT and *ypk1*Δ yeast (Fig. 2), suggesting that the difference in external GroPCho production is not due to increased PC synthesis but rather to altered patterns of turnover. This result also suggests that choline uptake was not significantly affected by loss of Ypk1, a suggestion substantiated by the fact that similar levels of incorporated label occurred in all strains following the radioactive pulse (data not shown).

In contrast, the Plb1 sequence lacks the Ypk1 consensus phosphorylation site. Furthermore, Plb1 was shown to have a low likelihood value for phosphorylation by Ypk1 in a large scale peptide screen for kinase activity (55). Similarly, the Plb1 sequence does not contain the Fpk1 phosphoacceptor site, R*X*SLDX_{15-21}R*X*SL*X*D (1). Thus, direct regulation of Plb1

through phosphorylation by Ypk1 or its downstream kinase, Fpk1, is unlikely. In addition, a strain bearing a deletion in *FPK1* did not significantly alter GroPCho production. The percentages of total [^{14}C]choline label incorporated into external GroPCho in the *fpk1*Δ and WT strains following an 8-h chase were 8 ± 1 and 5 ± 1%, respectively. Together, these data strongly suggest that Fpk1 is not involved in the regulation of Plb1 by Ypk1.

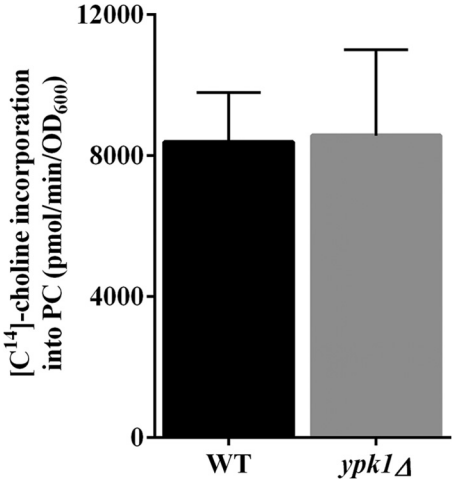

FIGURE 2. **Synthesis of PC is unaltered upon loss of Ypk1.** WT and *ypk1*Δ strains in the BY4742 background were grown to log phase, harvested, and resuspended to equal optical density in synthetic medium. [^{14}C]choline was added, and the amount of incorporation into PC after 30 min was determined. Values are the means ± S.E. (*error bars*) of three independent cultures assayed in duplicate. Similar results were observed in the YPH499 background (data not shown).

*The Secreted and Cell-associated Forms of Plb1 Increase in ypk1*Δ *Strain*—Plb1 activity has been reported in plasma membrane fractions, in the periplasm, and in the culture supernatant (19, 21). However, localization data were absent in large scale analyses using fluorescent tags fused to the C termini of yeast ORFs expressed under control of their endogenous promoters (56–60) and in a study utilizing C-terminal fusions to an epitope tag with the target genes expressed under control of the GAL promoter (61). In addition, a localization screen of proteins involved in lipid metabolism, in which Plb1 was C-terminally tagged and expressed under the control of the TEF promoter, demonstrated ER and vesicle localization, but plasma membrane localization was not apparent; the medium/secreted fraction was not analyzed in this study (62). Complicating the question of Plb1 localization is that it has a predicted GPI anchor, which should lead to plasma membrane residence (63, 64). During processing, GPI-anchored proteins are cleaved just after the anchor attachment site, which removes the C terminus (22). Therefore, if Plb1 were GPI-anchored, then C-terminal

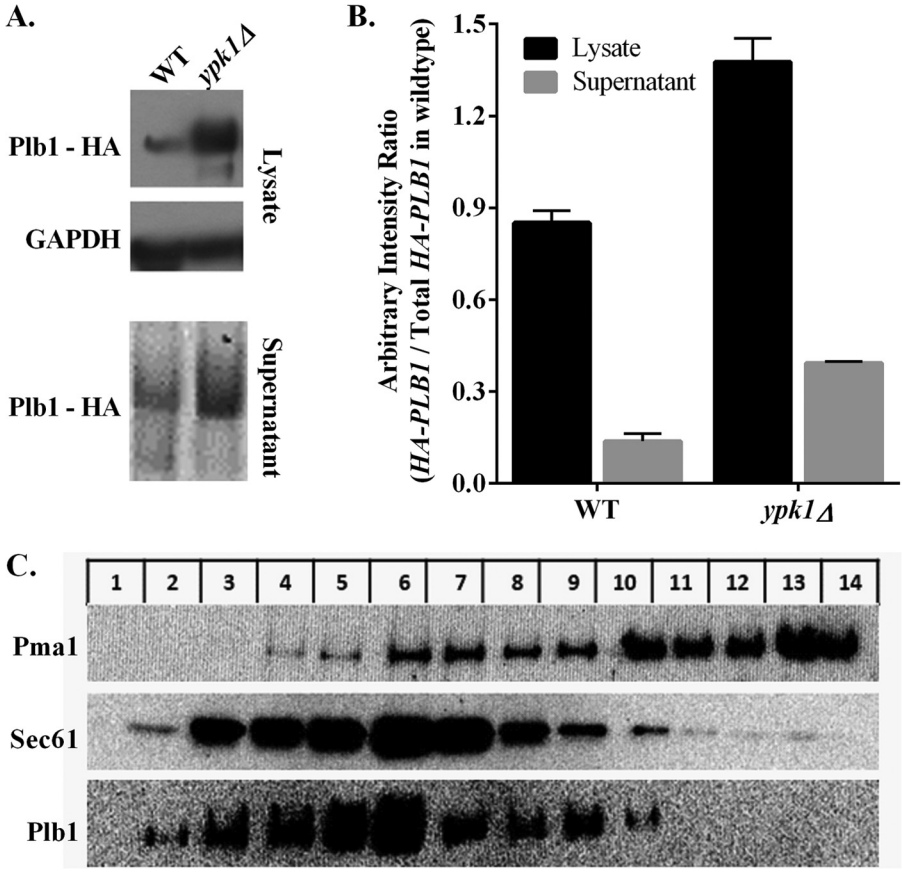

FIGURE 3. **Plb1 protein abundance and localization.** *A*, WT and *ypk1*Δ yeast containing the *PLB1-I-3xHA* allele were grown in synthetic medium at 30 °C to log phase. The supernatant was concentrated 100-fold, and total protein was extracted from the cells. A Western blot was performed on both fractions using an anti-HA-Plb1 primary antibody and HRP-conjugated anti-mouse secondary antibody. GAPDH was used as a loading control for the lysate fractions. *B*, the amount of Plb1 protein was quantified by densitometry of Western blots and normalized to the culture density (A_{600}) and sample volume. Values represent the fraction of total Plb1 protein in the WT strain. *C*, WT yeast containing *PLB1-I-3xHA* were grown in synthetic medium, lysed, and subjected to sucrose gradient centrifugation. The gradient was fractionated, and the migration of Plb1 and the indicated marker proteins, Pma1 (plasma membrane) and Sec61 (ER), were determined by SDS-PAGE and Western blot analysis. *Fraction number 1* on the *left* represents the top of the gradient. *Error bars*, S.E.

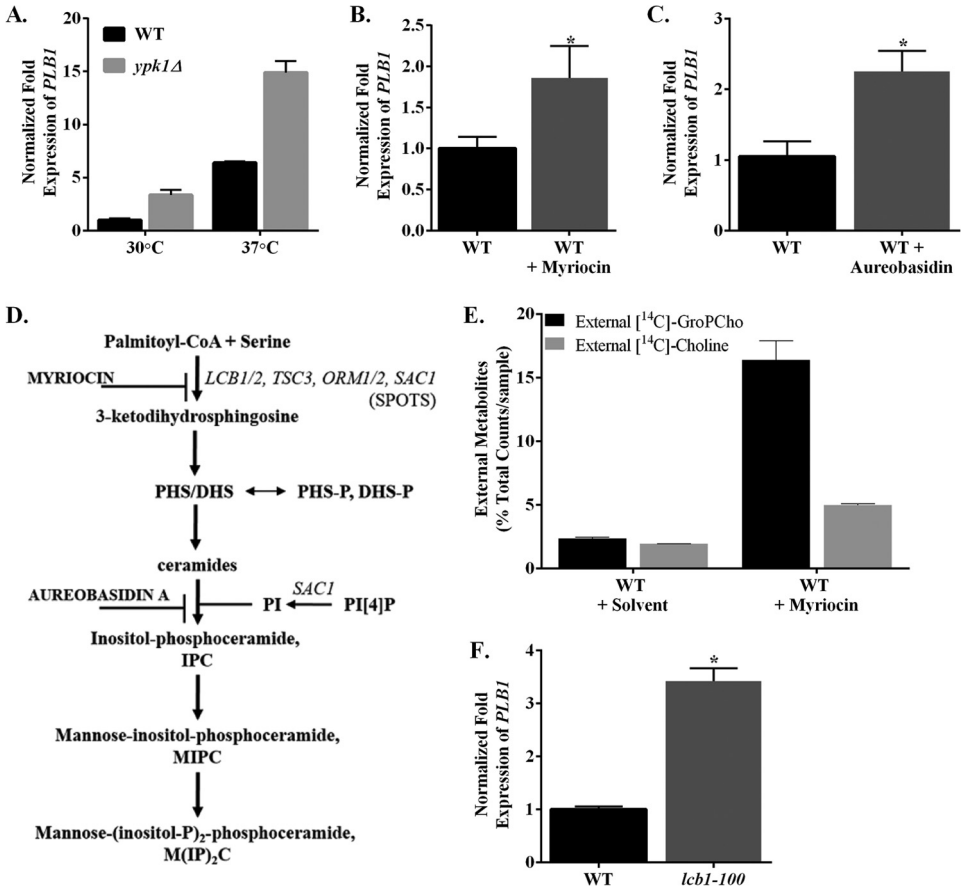

FIGURE 4. ***PLB1* message levels are elevated by heat stress and upon disruption of sphingolipid homeostasis.** *A*, strains in the BY4742 background were grown to early log phase in synthetic medium at 30 °C. Cultures were split and incubated at 30 or 37 °C, as indicated, for 3 h. *B*, cells were grown in synthetic medium at 30 °C to an A_{600} of ~0.7, myriocin (dissolved in methanol) was added to a final concentration of 1 μg/ml, and cultures were incubated for 2 h at 30 °C. *C*, cells were grown in synthetic medium at 30 °C to an A_{600} of ~0.4, aureobasidin (dissolved in methanol) was added to a final concentration of 1 μg/ml, and the cells were incubated for 3 h at 30 °C. *A–C*, after harvesting the cells, total RNA was extracted, and *PLB1* transcript levels were analyzed by real-time qRT-PCR using the comparative $\Delta\Delta C_T$ method. Data were normalized to the amount of the endogenous control mRNA, *SNR17*, and expressed relative to the value in WT control cells. Values represent the means ± S.E. (*error bars*) of at least three independent cultures assayed in triplicate. *D*, simplified schematic of sphingolipid synthesis in *S. cerevisiae* including targets of inhibiting drugs. *E*, WT cells in the BY4742 background were pregrown at 30 °C in synthetic medium containing 0.2 μCi/ml [^{14}C]choline chloride, followed by a chase at 30 °C in synthetic medium containing 10 mM choline and 1 μg/ml myriocin in methanol or an equivalent volume of methanol. Extracellular, intracellular, and membrane fractions were isolated, and [^{14}C]choline-containing metabolites from extracellular fractions after 3 h were separated by anion exchange chromatography. Values are the means ± S.E. of at least duplicate cultures and are representative of multiple experiments. Similar trends were observed in the YPH499 background (data not shown). *F*, the *lcb1-100* and WT strains were grown in synthetic medium at room temperature (25 °C) to an A_{600} of ~0.4 and then shifted to the restrictive temperature, 37 °C, for 90 min. RNA was extracted and analyzed as in *A–C*. Student's *t* test was performed for statistical analysis (*B*, $p = 0.05$; *C*, $p = 0.008$; *F*, $p = 0.0006$).

tagging, as used in several of the studies cited above, would be unable to detect the final processed protein.

To establish the localization of Plb1 and to have a reliable epitope-tagged Plb1 for Western analysis, we constructed a WT and *ypk1*Δ strain in which HA was inserted into the genomic copy of *PLB1* near the N-terminal end (*i.e.* after the signal sequence but before the catalytic site). This *PLB1-I-3xHA* construct was judged functional by confirming that *ypk1*Δ containing *PLB1-I-3xHA* displayed elevated GroPCho production indistinguishable from the *ypk1*Δ strain (see "Experimental Procedures"; data not shown). Consistent with increased GroPCho production, *ypk1*Δ containing the *PLB1-I-3xHA* allele displayed greater Plb1 abundance in total cell lysates and in the medium as compared with the WT strain (Fig. 3, *A* and *B*). To examine intracellular localization, we performed sucrose gradient fractionation using lysates from WT strains that contained the integrated, functional *PLB1-I-3xHA* gene. Interestingly, we found Plb1 associated with the ER (as indicated by co-migration with Sec61), as expected for a protein trafficking through the secretory pathway, but the protein was absent from plasma membrane fractions, as indicated by the migration of Pma1 (Fig. 3*C*). These results, which are consistent with fluorescence microscopy of C-terminally tagged Plb1 under the control of the TEF promoter (62), lead us to conclude that the protein is not plasma membrane-associated and that if it is GPI-anchored, it is readily released from the plasma membranes under the conditions used here. We suspect that the cell surface-associated Plb1 activity that releases GroPCho into the medium is due to its periplasmic localization.

Although Plb1 is predicted to be 72 kDa, the species found in the lysate migrates at ~145 kDa. Although the 145-kDa species is the most abundant form in the medium, a less abundant, diffuse band at ~260 kDa is also present. Plb1 is known to be *N*-glycosylated (65, 66), and multiple glycosylated orms of secreted phospholipase B have been detected previously (19, 67,

68). Upon treatment with Endo H_f, the protein migrates as one species at ~72 kDa (data not shown).

Compromised Sphingolipid Synthesis Up-regulates PLB1 Expression and Increases PC Turnover—Consistent with the observed increase in PC deacylation and Plb1 abundance (Figs. 1 and 3), *PLB1* transcript levels also increased upon loss of *YPK1* at both 30 °C and after a 37 °C temperature shift (Fig. 4*A*). In both WT and ypk1Δ yeast, a shift to 37 °C increased *PLB1* message levels. The *ypk1*Δ strain in the YPH499 background displayed a similar trend (data not shown).

The major role for Ypk1 described in the literature is the regulation of sphingolipid homeostasis (2). If the mechanism by which loss of Ypk1 up-regulates Plb1 expression involves compromised sphingolipid synthesis, we would expect reduction of sphingolipid synthesis by other means to have a similar effect on Plb1 expression. Indeed, *PLB1* expression was elevated in a WT strain treated with either myriocin or aureobasidin (Fig. 4, *B* and *C*), which inhibit SPT and inositol phosphoceramide synthase, respectively (69, 70) (Fig. 4*D*). We also monitored PC turnover in WT cells treated with myriocin and saw the expected increase in external GroPCho production (Fig. 4*E*). Similar trends were observed in a YPH499 strain background. Sphingolipid synthesis can also be diminished genetically through the use of the *lcb1-100* strain, which harbors temperature-sensitive SPT activity (71). As anticipated, the *lcb1-100* strain shifted to the restrictive temperature also exhibited increased *PLB1* expression as compared with WT (Fig. 4*F*).

The Crz1 Transcription Factor Is Responsible for PLB1 Up-regulation either When Sphingolipid Biosynthesis Is Compromised or When Ypk1 Is Absent—A recent microarray study showed that many of the up/down-regulated genes, including *PLB1*, identified in a *ypk1*Δ *ypk2*Δ strain bearing an inactivated analog-sensitive allele of *YPK1* (*YPK1*^{as}) contain binding sites for the Crz1 transcription factor (18, 19). Thus, we examined the role of Crz1 in mediating *PLB1* expression in response to altered sphingolipid biosynthesis or when *YPK1* was deleted. A *ypk1*Δ mutant exhibited increased *PLB1* message levels as compared with WT yeast, whereas *PLB1* message levels were unchanged in a *ypk1*Δ*crz1*Δ double mutant (Fig. 5*A*). In addition, up-regulation of *PLB1* expression in response to myriocin treatment (Fig. 4*B*) observed in a WT strain did not occur in the *crz1*Δ strain (Fig. 5*B*). These data indicate that Crz1 is required for the up-regulation of *PLB1* expression that occurs upon loss of Ypk1.

*Ameliorating Sphingolipid Synthesis by Deletion of ORM1 and ORM2 in a ypk1*Δ *Strain Returns PLB1 Expression and Extracellular GroPCho Production to WT Levels*—A primary mechanism by which Ypk1 regulates sphingolipid synthesis is through phosphorylation of Orm1 and Orm2 (17, 36). Orm1 and Orm2 are ER transmembrane proteins that regulate sphingolipid biosynthesis by binding to and inhibiting SPT (17, 18). Upon phosphorylation by Ypk1, the interaction between Orm1/2 and SPT is lessened, and sphingolipid biosynthesis is up-regulated. Thus, if Ypk1 regulates Plb1 via an Orm1/2-dependent effect on sphingolipid synthesis, we would expect *PLB1* expression to mirror WT levels in an *orm1*Δ*orm2*Δ*ypk1*Δ strain, as was found (Fig. 6*A*). Consistent with this result, a

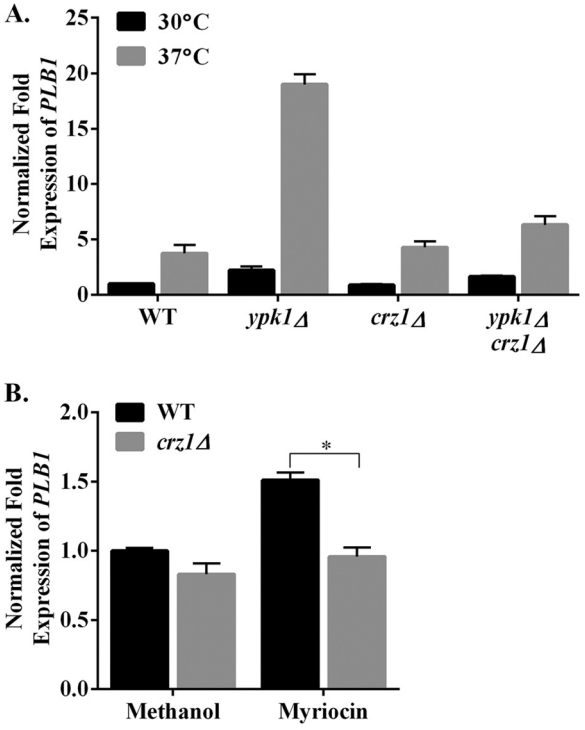

FIGURE 5. **Crz1 mediates *PLB1* up-regulation either when sphingolipid biosynthesis is compromised or when Ypk1 is absent.** *A*, strains (BY4742) were grown in synthetic medium at 30 °C to an A_{600} of ~0.7 (log phase). An aliquot was diluted to an A_{600} of ~0.2 and grown for 3 h at 37 °C. *B*, WT and *crz1*Δ strains were grown in synthetic medium at 30 °C to an A_{600} of ~0.7, myriocin (dissolved in methanol) was added to a final concentration of 1 μg/ml, and cells were incubated for 3.5 h at 30 °C. *A* and *B*, RNA was extracted, and *PLB1* message levels were analyzed by qRT-PCR using the comparative $\Delta\Delta C_T$ method. Data were normalized to the amount of the endogenous control mRNA, *SNR17*, and expressed relative to the value in WT cells grown at 30 °C (*A*) and WT cells grown with vehicle, methanol (*B*). Values represent the means ± S.E. (*error bars*) of three independent cultures assayed in triplicate. Student's *t* test was performed for statistical analysis; $p \leq 0.0001$.

*ypk1*Δ strain displays greater extracellular GroPCho production, but the levels of this metabolite nearly return to WT levels in the *orm1*Δ*orm2*Δ*ypk1*Δ strain (Fig. 6*B*).

To determine whether the Orm2 phosphorylation state regulates *PLB1* expression or GroPCho production, two other mutant strains, *orm1*Δ*orm2*^{Ala} (dephosphorylated mimic) and *orm1*Δ*orm2*^{Asp} (phosphorylated mimic), harboring or lacking the *YPK1* gene were employed. Specifically, these strains contain *ORM2* that is mutated to alanine or aspartic acid at the Ypk1 phosphorylation sites, Ser-46, Ser-47, and Ser-48, so they mimic the constitutively dephosphorylated or phosphorylated states (2, 36). These phosphorylation sites were shown to be immediately but transiently phosphorylated in response to heat stress in a Ypk1-dependent manner (36). Orm2 has also been shown to be the major Orm species based upon its greater expression than Orm1 and because only the *orm2*Δ strain displays a growth defect (36). In our experiments, performed over the course of several h, the *orm1*Δ*orm2*Δ, *orm1*Δ*orm2*^{Ala}, and *orm1*Δ*orm2*^{Asp} strains all have similar *PLB1* message levels and extracellular GroPCho production as compared with the WT strain (Fig. 6, *A* and *B*). In addition, the *orm1*Δ*orm2*^{Asp}*ypk1*Δ strain behaves similarly to the *ypk1*Δ strain. These results suggest that Orm2 phosphorylation at these specific amino acids is

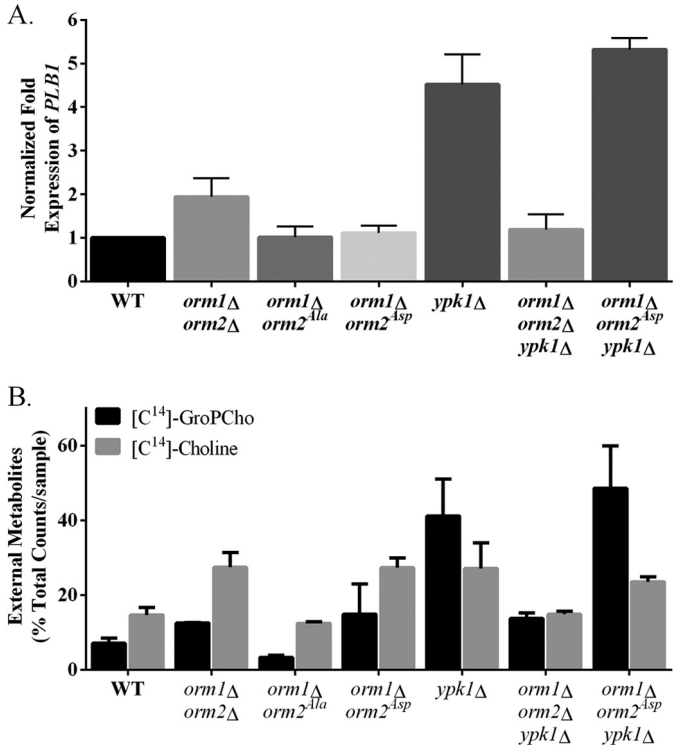

FIGURE 6. **Deletion of *ORM1* and *ORM2* in a *ypk1*Δ strain background reduces both *PLB1* expression and external GroPCho production.** *A*, cells in the DDY904 background were grown to log phase in synthetic medium at 30 °C and harvested. Total RNA was extracted, and *PLB1* transcript levels were analyzed by real-time qRT-PCR using the comparative $\Delta\Delta C_T$ method. Data were normalized to the amount of the endogenous control mRNA, *SNR17*, and expressed relative to the value in WT cells. Values represent the means ± S.E. of three independent cultures assayed in triplicate. *B*, cells were grown to log phase at 30 °C in synthetic medium containing 0.2 μCi/ml [^{14}C]choline chloride, followed by a chase at 37 °C in YNB medium containing 10 mM choline. Extracellular, intracellular, and membrane fractions were isolated, and [^{14}C]choline-containing metabolites from extracellular fractions were separated by anion exchange column chromatography. Values are the means ± S.E. (*error bars*) of triplicate cultures.

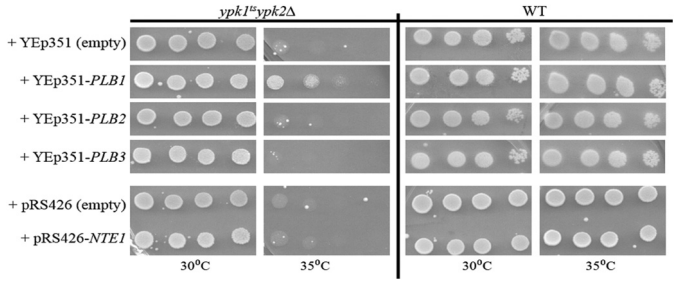

FIGURE 7. **Overexpression of only *PLB1* rescues the lethality of the *ypk1*^{ts}*ypk2*Δ strain at a restrictive temperature.** WT and *ypk1*^{ts}*ypk2*Δ strains (YPH499) harboring the indicated plasmids were pregrown in selective medium, harvested, and resuspended to equivalent densities. Cells from 5-fold serial dilutions of each culture were spotted onto selective medium and grown for 3 days at the permissive (30 °C) and restrictive (35 °C) temperatures.

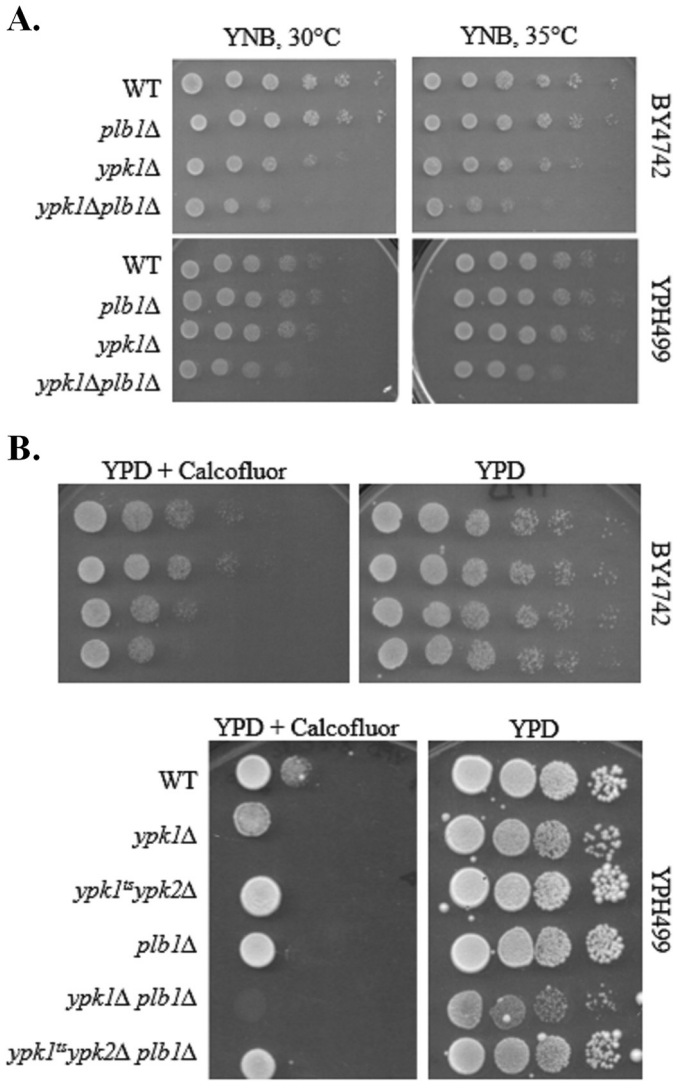

FIGURE 8. **The slowed growth phenotype and sensitivity to the cell wall perturbing agent, calcofluor white, in a *ypk1*Δ strain is exacerbated by deletion of *PLB1*.** *A*, strains in the BY4742 and YPH499 backgrounds were pregrown in synthetic medium, harvested, and resuspended to equivalent densities. Cells from 5-fold serial dilutions were spotted onto synthetic plates and incubated for 48 (BY4742) or 32 h (YPH499). *B*, WT and deletion strains were pregrown in synthetic medium, harvested, and resuspended to equivalent densities. 5-fold (BY4742) or 10-fold (YPH499) dilutions were spotted onto YPD and YPD + 8.5 μg/ml calcofluor white plates and incubated at 30 °C for 32 or 48 h, respectively. Data displayed are representative of multiple experiments.

not crucial for *PLB1* expression or PC turnover but that the Orm2 protein itself is required.

Overexpression of only PLB1 rescues *ypk1*^{ts}*ypk2*Δ lethality at the restrictive temperature. Plb1 was previously identified as a multicopy suppressor of lethality in the *ypk1*^{ts}Δ strain at the restrictive temperature of 37 °C (6). To determine whether rescue was *PLB1*-specific or could be conferred by other PLB-encoding genes, growth was monitored in the *ypk1*^{ts}*ypk2*Δ strain overexpressing *PLB1*, *PLB2*, *PLB3*, or *NTE1*. The genes were expressed from their endogenous promoters on multicopy plasmids (see "Experimental Procedures"). Although there was a 200–300-fold increase in *PLB1*, *PLB2*, and *PLB3* message levels and a 50-fold increase in *NTE1* message levels, only overexpression of *PLB1* rescued *ypk1*^{ts}*ypk2*Δ lethality at the restrictive temperature (Fig. 7).

Deletion of Both PLB1 and YPK1 Leads to Synthetic Interactions—Based on the data presented in Fig. 7, *PLB1* and *YPK1* appear to genetically interact. To confirm this hypothesis, we examined specific phenotypes in strains lacking both genes. As shown in Fig. 8*A*, a negative genetic interaction was observed between *YPK1* and *PLB1* when growth was monitored,

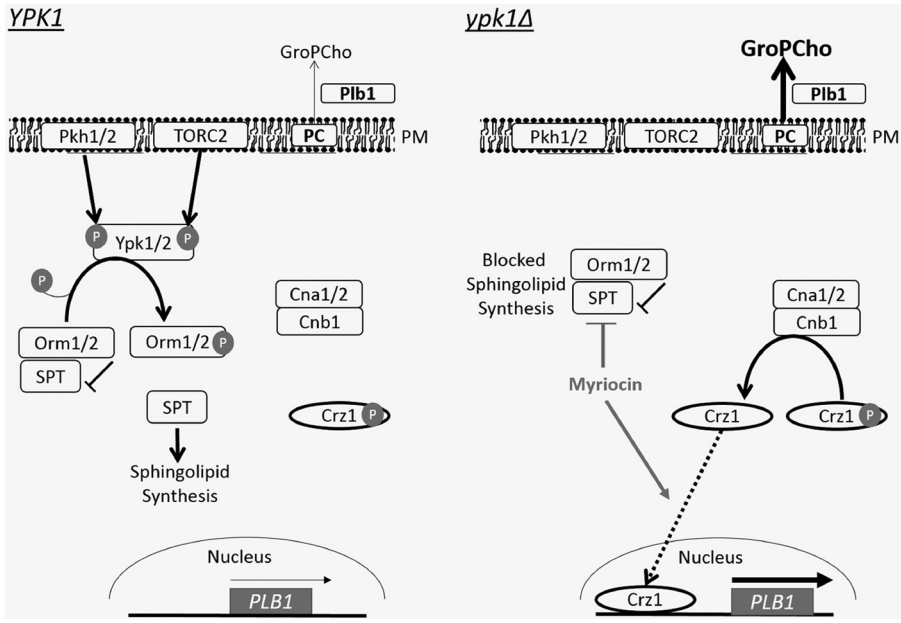

FIGURE 9. **Model of *PLB1* transcriptional activation upon loss of Ypk1 or upon disruption to sphingolipid biosynthesis through treatment with myriocin.** *Left*, events occurring in a WT cell in which cell growth is favored. TORC2 and Pkh1/2 phosphorylate and activate Ypk1, which leads to phosphorylation of Orm1/2 and subsequent release from SPT inhibition. This allows sphingolipid synthesis to proceed. The TORC2/Ypk1 signaling pathway predominates over the calcineurin pathway, resulting in only a basal level of *PLB1* transcription and a basal level of Plb1-mediated PC turnover. *Right*, events occurring under conditions promoting cell survival upon loss of *YPK1*, where the calcineurin signaling pathway predominates and Crz1 is dephosphorylated. Crz1 translocates into the nucleus and elevates *PLB1* transcript levels and Plb1-mediated PC turnover. The *right panel* (*gray lines*) also indicates elevation of Crz1-activated *PLB1* transcription in the presence of myriocin. The *dotted line* indicates movement into the nucleus. *PM*, plasma membrane.

although the severity of the defect varied somewhat depending upon the strain background employed. On solid synthetic medium, *ypk1*Δ*plb1*Δ isolates constructed in both the BY4742 or YPH499 backgrounds displayed a growth defect as compared with *ypk1*Δ at 30 and 35 °C (Fig. 8*A*). The *ypk1*Δ*plb1*Δ strain constructed in the YPH499 background also exhibited a growth defect on YPD plates (Fig. 8*B*).

The Ypk1 pathway influences several downstream events, including cell wall integrity (6, 7). Therefore, we examined the effect of the cell wall-perturbing agent, calcofluor white, on growth. A *ypk1*Δ*plb1*Δ mutant exhibited increased sensitivity to calcofluor white as compared with a *ypk1*Δ strain (Fig. 8*B*). This result was most striking in the YPH499 background, where no growth was observed in the *ypk1*Δ*plb1*Δ strain in the presence of calcofluor white when present at a final concentration of 8.5 μg/ml. These findings, together with the fact that *PLB1* is a multicopy suppressor of the lethality of $ypk1^{ts}ypk2\Delta$ yeast, indicate that increased PC turnover via Plb1 activity increases the fitness of cells when Ypk1 is absent. More generally, these findings suggest that sphingolipid synthesis is coordinated with PC turnover to maintain optimal lipid homeostasis.

DISCUSSION

PC is the most abundant glycerophospholipid in eukaryotic membranes, and its synthesis and catabolism are tightly regulated. In yeast, the known routes of PC catabolism occur through the action of the phospholipase D encoded by *PLD1/SPO14* (54), the ER-localized PLB encoded by *NTE1* (22), and *PLB1* (19). Here we show that Plb1 activity (Fig. 1) and expression (Figs. 4 and 5) were modulated by the serine/threonine kinase Ypk1. Furthermore, we show that regulation occurs via a mechanism in which the cell can detect compromised sphingolipid biosynthesis (Fig. 5). Blockage of SPT activity through use of an *lcb1-100* mutant or by treatment with myriocin also results in increased *PLB1* expression. Treatment of cells with aureobasidin A, which blocks downstream steps in the sphingolipid biosynthetic pathway, led to a similar effect, indicating that the formation of the complex sphingolipid, inositol phosphoceramide, at a minimum, is required to regulate *PLB1* (Fig. 5*D*).

Plb1 has been widely accepted as a secreted and plasma membrane-associated protein based on cellular fractionation studies and based on its role in the production of extracellular GroPCho (19). Our results, utilizing a Plb1 construct with an internal HA tag to account for a potential GPI anchor, indicate that Plb1 is secreted (Fig. 4*A*) and fractionates with the ER marker, Sec61, but not with the plasma membrane marker, Pma1 (Fig. 4*C*). As a secreted and glycosylated protein, it is not unexpected to find Plb1 at the ER. However, our data along with the data of others suggest the intriguing possibility that Plb1 may be active intracellularly as well as at the cell surface, because it has been shown to metabolize excess intracellular lysophospholipids (72) and to be involved in PC acyl chain remodeling (73). The secreted/periplasmic form of Plb1 is most likely responsible for the production of extracellular GroPCho. Notably, extracellular GroPCho is not a dead end metabolite but can be recycled into PC synthesis following its uptake via glycerophosphodiester transporters that have been identified in both *S. cerevisiae* (74) and *Candida albicans* (46, 75).

Ypk1 regulates sphingolipid synthesis by phosphorylating Orm1/2 (2). Phosphorylated Orm1/2 cannot bind to SPT, which results in up-regulated sphingolipid synthesis. Our results show that the increase in *PLB1* expression observed in a

*ypk1*Δ strain is mediated by Orm1/2, because *PLB1* transcript levels are depressed to WT levels in the *orm1*Δ*orm2*Δ*ypk1*Δ strain (Fig. 6). Whereas the Orm1/2 proteins trigger the increased *PLB1* response upon loss of *YPK1,* we find that the phosphorylation state of Orm2 at residues Ser-46, Ser-47, and Ser-48 is not involved in controlling *PLB1* expression or PC turnover. Interestingly, Orm1 and Orm2 have also been found to physically interact with the ceramide synthase subunit, Lac1, suggesting that Orm1/2 regulate the sphingolipid biosynthetic pathway at multiple steps (76). These data suggest a complicated relationship between Orm1/2 and its role in regulating sphingolipid and phospholipid metabolism.

Phosphorylation of the lipid flippase activator, Fpk1, by Ypk1 down-regulates the Dnf1 and Dnf2 flippases (1). In addition, Fpk1 has been linked to elevated levels of reactive oxygen species that are produced upon loss of Ypk1 (13). Our results do not indicate a connection between Plb1 activity and Fpk1, because an *fpk1*Δ strain does not display increased PC turnover, and Plb1 lacks a Fpk1/2 phosphoacceptor site.

We also discovered that the calcineurin-dependent responsive element-associated transcription factor, Crz1, is a key regulator of the increased *PLB1* expression observed upon disruption of sphingolipid biosynthesis. Interestingly, Crz1 is not responsible for increased *PLB1* transcription observed upon heat stress (Fig. 6*A*), suggesting multiple levels of *PLB1* regulation, depending on the applied stress. Consistent with our findings, a *ypk1*Δ*ypk2*Δ strain bearing a *YPK1*^{as} allele displays increased expression of several genes, many that have Crz1 binding sites in their promoters, including *PLB1* (10). Also, others have shown that disruption of sphingolipid synthesis leads to increased expression of *PMC1*, which is a calcineurin-dependent gene (77). Based on these and other data, a model was proposed (10) in which the TORC2 and calcineurin pathways act antagonistically to maintain the optimal cell growth and survival. When Ypk1 is recruited to the plasma membrane by Slm1/2, there is a shift toward down-regulation of the calcineurin pathway and up-regulation of TORC2 signaling. Therefore, in a *ypk1*Δ strain, activation of the calcineurin pathway would predominate, activating the downstream transcription factor, Crz1, which in turn activates various calcineurin-dependent responsive element-containing genes, including *PLB1* (Fig. 9). Interestingly, treatment of cells with myriocin results in TORC2-dependent phosphorylation of Ypk1 in a manner that requires the Ypk1-recruiting proteins, Slm1/2, to translocate from eisosomes to membrane compartments containing TOR (11, 12). Because Slm1 relocalization was suggested to be a result of an altered sphingolipid environment and an increase in reactive oxygen species (13), it is tempting to speculate that alterations in the eisosome lipid environment due to Plb1-mediated PC turnover may also contribute to Slm1 relocalization.

Our phenotypic analysis of the *ypk1*Δ*plb1*Δ double mutant suggests that up-regulated Plb1 activity upon loss of Ypk1 is a functionally important compensatory mechanism, because slowed growth and sensitivity to calcofluor white are exacerbated upon deletion of *PLB1* in the *ypk1*Δ strain (Fig. 8). Two lines of evidence indicate Plb1 activity, as opposed to activity of the other PLBs, mediates this phenomenon: 1) only overexpression of *PLB1* rescues growth of the *ypk1*^{ts}*ypk2*Δ strain at a restrictive temperature (Fig. 8), and 2) turnover of PI, the primary substrate of Plb3, is unaltered in the *ypk1*Δ strain. The mechanism by which Plb1 activity rescues phenotypes associated with loss of the Ypk1/2 proteins has not been elucidated and will be the focus of future work. However, one possibility is that PC levels, which are in turn modulated through Plb1 activity, affect the activities of essential plasma membrane proteins. It is also possible that the metabolic products of Plb1, GroPCho and free fatty acids, are responsible for the rescued phenotypes. Alternatively, as others have suggested, overexpression of *PLB1* could induce greater damage to cell wall integrity, resulting in activation of additional cell wall integrity recovery pathways to facilitate rescue (6).

In summary, our results indicate that Ypk1, in addition to regulating sphingolipid synthesis and plasma membrane flippase activity, also regulates the turnover of the major phospholipid, PC. Future studies will focus on the mechanism by which altered sphingolipid biosynthesis, as engendered by loss of Ypk1, activates the myriad genes under the control of Crz1, such as Plb1.

Acknowledgments—We thank Jeremy Thorner, David Drubin, and Yusef Hannun for the gifts of yeast strains and Nancy Hollingsworth, Susan Henry, and Chris McMaster for the gifts of plasmids.

REFERENCES

1. Roelants, F. M., Baltz, A. G., Trott, A. E., Fereres, S., and Thorner, J. (2010) A protein kinase network regulates the function of aminophospholipid flippases. *Proc. Natl. Acad. Sci. U.S.A.* **107,** 34–39
2. Roelants, F. M., Breslow, D. K., Muir, A., Weissman, J. S., and Thorner, J. (2011) Protein kinase Ypk1 phosphorylates regulatory proteins Orm1 and Orm2 to control sphingolipid homeostasis in *Saccharomyces cerevisiae*. *Proc. Natl. Acad. Sci. U.S.A.* **108,** 19222–19227
3. Tanoue, D., Kobayashi, T., Sun, Y., Fujita, T., Takematsu, H., and Kozutsumi, Y. (2005) The requirement for the hydrophobic motif phosphorylation of Ypk1 in yeast differs depending on the downstream events, including endocytosis, cell growth, and resistance to a sphingolipid biosynthesis inhibitor, ISP-1. *Arch. Biochem. Biophys.* **437,** 29–41
4. Sun, Y., Taniguchi, R., Tanoue, D., Yamaji, T., Takematsu, H., Mori, K., Fujita, T., Kawasaki, T., and Kozutsumi, Y. (2000) Sli2 (Ypk1), a homologue of mammalian protein kinase SGK, is a downstream kinase in the sphingolipid-mediated signaling pathway of yeast. *Mol. Cell Biol.* **20,** 4411–4419
5. Li, X., Gianoulis, T. A., Yip, K. Y., Gerstein, M., and Snyder, M. (2010) Extensive *in vivo* metabolite-protein interactions revealed by large-scale systematic analyses. *Cell* **143,** 639–650
6. Roelants, F. M., Torrance, P. D., Bezman, N., and Thorner, J. (2002) Pkh1 and Pkh2 differentially phosphorylate and activate Ypk1 and Ykr2 and define protein kinase modules required for maintenance of cell wall integrity. *Mol. Biol. Cell* **13,** 3005–3028
7. Schmelzle, T., Helliwell, S. B., and Hall, M. N. (2002) Yeast protein kinases and the *RHO1* exchange factor *TUS1* are novel components of the cell integrity pathway in yeast. *Mol. Cell. Biol.* **22,** 1329–1339
8. Jacquier, N., and Schneiter, R. (2010) Ypk1, the yeast orthologue of the human serum- and glucocorticoid-induced kinase, is required for efficient uptake of fatty acids. *J. Cell Sci.* **123,** 2218–2227
9. Casamayor, A., Torrance, P. D., Kobayashi, T., Thorner, J., and Alessi, D. R. (1999) Functional counterparts of mammalian protein kinases PDK1 and SGK in budding yeast. *Curr. Biol.* **9,** 186–197
10. Niles, B. J., Mogri, H., Hill, A., Vlahakis, A., and Powers, T. (2012) Plasma membrane recruitment and activation of the AGC kinase Ypk1 is mediated by target of rapamycin complex 2 (TORC2) and its effector proteins Slm1 and Slm2. *Proc. Natl. Acad. Sci. U.S.A.* **109,** 1536–1541

11. Niles, B. J., and Powers, T. (2012) Plasma membrane proteins Slm1 and Slm2 mediate activation of the AGC kinase Ypk1 by TORC2 and sphingolipids in *S. cerevisiae*. *Cell Cycle* **11,** 3745–3749
12. Berchtold, D., Piccolis, M., Chiaruttini, N., Riezman, I., Riezman, H., Roux, A., Walther, T. C., and Loewith, R. (2012) Plasma membrane stress induces relocalization of Slm proteins and activation of TORC2 to promote sphingolipid synthesis. *Nat. Cell Biol.* **14,** 542–547
13. Niles, B. J., Joslin, A. C., Fresques, T., and Powers, T. (2014) TOR complex 2-Ypk1 signaling maintains sphingolipid homeostasis by sensing and regulating ROS accumulation. *Cell Rep.* **6,** 541–552
14. Friant, S., Lombardi, R., Schmelzle, T., Hall, M. N., and Riezman, H. (2001) Sphingoid base signaling via Pkh kinases is required for endocytosis in yeast. *EMBO J.* **20,** 6783–6792
15. Lee, Y. J., Jeschke, G. R., Roelants, F. M., Thorner, J., and Turk, B. E. (2012) Reciprocal phosphorylation of yeast glycerol-3-phosphate dehydrogenases in adaptation to distinct types of stress. *Mol. Cell. Biol.* **32,** 4705–4717
16. Nakano, K., Yamamoto, T., Kishimoto, T., Noji, T., and Tanaka, K. (2008) Protein kinases Fpk1p and Fpk2p are novel regulators of phospholipid asymmetry. *Mol. Biol. Cell* **19,** 1783–1797
17. Breslow, D. K., Collins, S. R., Bodenmiller, B., Aebersold, R., Simons, K., Shevchenko, A., Ejsing, C. S., and Weissman, J. S. (2010) Orm family proteins mediate sphingolipid homeostasis. *Nature* **463,** 1048–1053
18. Han, S., Lone, M. A., Schneiter, R., and Chang, A. (2010) Orm1 and Orm2 are conserved endoplasmic reticulum membrane proteins regulating lipid homeostasis and protein quality control. *Proc. Natl. Acad. Sci. U.S.A.* **107,** 5851–5856
19. Lee, K. S., Patton, J. L., Fido, M., Hines, L. K., Kohlwein, S. D., Paltauf, F., Henry, S. A., and Levin, D. E. (1994) The *Saccharomyces cerevisiae PLB1* gene encodes a protein required for lysophospholipase and phospholipase B activity. *J. Biol. Chem.* **269,** 19725–19730
20. Patton-Vogt, J. (2007) Transport and metabolism of glycerophosphodiesters produced through phospholipid deacylation. *Biochim. Biophys. Acta* **1771,** 337–342
21. Merkel, O., Fido, M., Mayr, J. A., Prüger, H., Raab, F., Zandonella, G., Kohlwein, S. D., and Paltauf, F. (1999) Characterization and function *in vivo* of two novel phospholipases B/lysophospholipases from *Saccharomyces cerevisiae*. *J. Biol. Chem.* **274,** 28121–28127
22. Zaccheo, O., Dinsdale, D., Meacock, P. A., and Glynn, P. (2004) Neuropathy target esterase and its yeast homologue degrade phosphatidylcholine to glycerophosphocholine in living cells. *J. Biol. Chem.* **279,** 24024–24033
23. Henry, S. A., Kohlwein, S. D., and Carman, G. M. (2012) Metabolism and regulation of glycerolipids in the yeast *Saccharomyces cerevisiae*. *Genetics* **190,** 317–349
24. Fagone, P., and Jackowski, S. (2013) Phosphatidylcholine and the CDP-choline cycle. *Biochim. Biophys. Acta* **1831,** 523–532
25. Yoshimoto, M., Waki, A., Obata, A., Furukawa, T., Yonekura, Y., and Fujibayashi, Y. (2004) Radiolabeled choline as a proliferation marker: comparison with radiolabeled acetate. *Nucl. Med. Biol.* **31,** 859–865
26. Sanchez-Lopez, E., Zimmerman, T., Gomez del Pulgar, T., Moyer, M. P., Lacal Sanjuan, J. C., and Cebrian, A. (2013) Choline kinase inhibition induces exacerbated endoplasmic reticulum stress and triggers apoptosis via CHOP in cancer cells. *Cell Death Dis.* **4,** e933
27. Kurabe, N., Hayasaka, T., Ogawa, M., Masaki, N., Ide, Y., Waki, M., Nakamura, T., Kurachi, K., Kahyo, T., Shinmura, K., Midorikawa, Y., Sugiyama, Y., Setou, M., and Sugimura, H. (2013) Accumulated phosphatidylcholine (16:0/16:1) in human colorectal cancer: possible involvement of LPCAT4. *Cancer Sci.* **104,** 1295–1302
28. Zhou, X., Mao, J., Ai, J., Deng, Y., Roth, M. R., Pound, C., Henegar, J., Welti, R., and Bigler, S. A. (2012) Identification of plasma lipid biomarkers for prostate cancer by lipidomics and bioinformatics. *PloS One* **7,** e48889
29. Whiley, L., Sen, A., Heaton, J., Proitsi, P., García-Gómez, D., Leung, R., Smith, N., Thambisetty, M., Kloszewska, I., Mecocci, P., Soininen, H., Tsolaki, M., Vellas, B., Lovestone, S., Legido-Quigley, C., and AddNeuroMed Consortium (2014) Evidence of altered phosphatidylcholine metabolism in Alzheimer's disease. *Neurobiol. Aging* **35,** 271–278
30. Fonteh, A. N., Chiang, J., Cipolla, M., Hale, J., Diallo, F., Chirino, A., Arakaki, X., and Harrington, M. G. (2013) Alterations in cerebrospinal fluid glycerophospholipids and phospholipase A2 activity in Alzheimer's disease. *J. Lipid Res.* **54,** 2884–2897
31. Fernández-Murray, J. P., and McMaster, C. R. (2005) Glycerophosphocholine catabolism as a new route for choline formation for phosphatidylcholine synthesis by the Kennedy pathway. *J. Biol. Chem.* **280,** 38290–38296
32. Patton, J. L., Pessoa-Brandao, L., and Henry, S. A. (1995) Production and reutilization of an extracellular phosphatidylinositol catabolite, glycerophosphoinositol, by *Saccharomyces cerevisiae*. *J. Bacteriol.* **177,** 3379–3385
33. Longtine, M. S., McKenzie, A., 3rd, Demarini, D. J., Shah, N. G., Wach, A., Brachat, A., Philippsen, P., and Pringle, J. R. (1998) Additional modules for versatile and economical PCR-based gene deletion and modification in *Saccharomyces cerevisiae*. *Yeast* **14,** 953–961
34. Goldstein, A. L., and McCusker, J. H. (1999) Three new dominant drug resistance cassettes for gene disruption in *Saccharomyces cerevisiae*. *Yeast* **15,** 1541–1553
35. Güldener, U., Heck, S., Fielder, T., Beinhauer, J., and Hegemann, J. H. (1996) A new efficient gene disruption cassette for repeated use in budding yeast. *Nucleic Acids Res.* **24,** 2519–2524
36. Sun, Y., Miao, Y., Yamane, Y., Zhang, C., Shokat, K. M., Takematsu, H., Kozutsumi, Y., and Drubin, D. G. (2012) Orm protein phosphoregulation mediates transient sphingolipid biosynthesis response to heat stress via the Pkh-Ypk and Cdc55-PP2A pathways. *Mol. Biol. Cell* **23,** 2388–2398
37. Schneider, B. L., Seufert, W., Steiner, B., Yang, Q. H., and Futcher, A. B. (1995) Use of polymerase chain reaction epitope tagging for protein tagging in *Saccharomyces cerevisiae*. *Yeast* **11,** 1265–1274
38. Dowd, S. R., Bier, M. E., and Patton-Vogt, J. L. (2001) Turnover of phosphatidylcholine in *Saccharomyces cerevisiae*: the role of the CDP-choline pathway. *J. Biol. Chem.* **276,** 3756–3763
39. Cook, S. J., and Wakelam, M. J. (1989) Analysis of the water-soluble products of phosphatidylcholine breakdown by ion-exchange chromatography. Bombesin and TPA (12-*O*-tetradecanoylphorbol 13-acetate) stimulate choline generation in Swiss 3T3 cells by a common mechanism. *Biochem. J.* **263,** 581–587
40. Martin, T. W. (1988) Formation of diacylglycerol by a phospholipase D-phosphatidate phosphatase pathway specific for phosphatidylcholine in endothelial cells. *Biochim. Biophys. Acta* **962,** 282–296
41. Fisher, E., Almaguer, C., Holic, R., Griac, P., and Patton-Vogt, J. (2005) Glycerophosphocholine-dependent growth requires Gde1p (YPL110c) and Git1p in *Saccharomyces cerevisiae*. *J. Biol. Chem.* **280,** 36110–36117
42. Zheng, B., Berrie, C. P., Corda, D., and Farquhar, M. G. (2003) GDE1/MIR16 is a glycerophosphoinositol phosphodiesterase regulated by stimulation of G protein-coupled receptors. *Proc. Natl. Acad. Sci. U.S.A.* **100,** 1745–1750
43. Hanson, B. A., and Lester, R. L. (1980) The extraction of inositol-containing phospholipids and phosphatidylcholine from *Saccharomyces cerevisiae* and *Neurospora crassa*. *J. Lipid Res.* **21,** 309–315
44. Vaden, D. L., Gohil, V. M., Gu, Z., and Greenberg, M. L. (2005) Separation of yeast phospholipids using one-dimensional thin-layer chromatography. *Anal. Biochem.* **338,** 162–164
45. Sun, T., Wetzel, S. J., Johnson, M. E., Surlow, B. A., and Patton-Vogt, J. (2012) Development and validation of a hydrophilic interaction liquid chromatography-tandem mass spectrometry method for the quantification of lipid-related extracellular metabolites in *Saccharomyces cerevisiae*. *J. Chromatogr. B Analyt. Technol. Biomed. Life Sci.* **897,** 1–9
46. Bishop, A. C., Sun, T., Johnson, M. E., Bruno, V. M., and Patton-Vogt, J. (2011) Robust utilization of phospholipase-generated metabolites, glycerophosphodiesters, by *Candida albicans*: role of the CaGit1 permease. *Eukaryot. Cell* **10,** 1618–1627
47. Ausubel, F. M., Brent, R., Kingston, R. E., Moore, D. D., Seideman, J. G., Smith, J. A., and Struhl, K. (1999) *Short Protocols in Molecular Biology*, pp. 13-1–13-57, John Wiley and Sons Inc., New York
48. Livak, K. J., and Schmittgen, T. D. (2001) Analysis of relative gene expression data using real-time quantitative PCR and the $2(-\Delta\Delta C(T))$ method. *Methods* **25,** 402–408
49. Pfaffl, M. W. (2001) A new mathematical model for relative quantification in real-time RT-PCR. *Nucleic Acids Res.* **29,** e45
50. Sullivan, M. L., Youker, R. T., Watkins, S. C., and Brodsky, J. L. (2003)

Localization of the BiP molecular chaperone with respect to endoplasmic reticulum foci containing the cystic fibrosis transmembrane conductance regulator in yeast. *J. Histochem. Cytochem.* **51,** 545–548
51. Kolb, A. R., Needham, P. G., Rothenberg, C., Guerriero, C. J., Welling, P. A., and Brodsky, J. L. (2014) ESCRT regulates surface expression of the Kir2.1 potassium channel. *Mol. Biol. Cell* **25,** 276–289
52. Stirling, C. J., Rothblatt, J., Hosobuchi, M., Deshaies, R., and Schekman, R. (1992) Protein translocation mutants defective in the insertion of integral membrane proteins into the endoplasmic reticulum. *Mol. Biol. Cell* **3,** 129–142
53. Dickson, R. C., Sumanasekera, C., and Lester, R. L. (2006) Functions and metabolism of sphingolipids in *Saccharomyces cerevisiae*. *Prog. Lipid Res.* **45,** 447–465
54. Waksman, M., Eli, Y., Liscovitch, M., and Gerst, J. E. (1996) Identification and characterization of a gene encoding phospholipase D activity in yeast. *J. Biol. Chem.* **271,** 2361–2364
55. Mok, J., Kim, P. M., Lam, H. Y., Piccirillo, S., Zhou, X., Jeschke, G. R., Sheridan, D. L., Parker, S. A., Desai, V., Jwa, M., Cameroni, E., Niu, H., Good, M., Remenyi, A., Ma, J. L., Sheu, Y. J., Sassi, H. E., Sopko, R., Chan, C. S., De Virgilio, C., Hollingsworth, N. M., Lim, W. A., Stern, D. F., Stillman, B., Andrews, B. J., Gerstein, M. B., Snyder, M., and Turk, B. E. (2010) Deciphering protein kinase specificity through large-scale analysis of yeast phosphorylation site motifs. *Sci. Signal.* **3,** ra12
56. Habeler, G., Natter, K., Thallinger, G. G., Crawford, M. E., Kohlwein, S. D., and Trajanoski, Z. (2002) YPL.db: the yeast protein localization database. *Nucleic Acids Res.* **30,** 80–83
57. Kals, M., Natter, K., Thallinger, G. G., Trajanoski, Z., and Kohlwein, S. D. (2005) YPL.db2: the yeast protein localization database, version 2.0. *Yeast* **22,** 213–218
58. Huh, W. K., Falvo, J. V., Gerke, L. C., Carroll, A. S., Howson, R. W., Weissman, J. S., and O'Shea, E. K. (2003) Global analysis of protein localization in budding yeast. *Nature* **425,** 686–691
59. Ghaemmaghami, S., Huh, W. K., Bower, K., Howson, R. W., Belle, A., Dephoure, N., O'Shea, E. K., and Weissman, J. S. (2003) Global analysis of protein expression in yeast. *Nature* **425,** 737–741
60. Howson, R., Huh, W. K., Ghaemmaghami, S., Falvo, J. V., Bower, K., Belle, A., Dephoure, N., Wykoff, D. D., Weissman, J. S., and O'Shea, E. K. (2005) Construction, verification and experimental use of two epitope-tagged collections of budding yeast strains. *Comp. Funct. Genomics* **6,** 2–16
61. Kumar, A., Agarwal, S., Heyman, J. A., Matson, S., Heidtman, M., Piccirillo, S., Umansky, L., Drawid, A., Jansen, R., Liu, Y., Cheung, K. H., Miller, P., Gerstein, M., Roeder, G. S., and Snyder, M. (2002) Subcellular localization of the yeast proteome. *Genes Dev.* **16,** 707–719
62. Natter, K., Leitner, P., Faschinger, A., Wolinski, H., McCraith, S., Fields, S., and Kohlwein, S. D. (2005) The spatial organization of lipid synthesis in the yeast *Saccharomyces cerevisiae* derived from large scale green fluorescent protein tagging and high resolution microscopy. *Mol. Cell. Proteomics* **4,** 662–672
63. Hamada, K., Terashima, H., Arisawa, M., Yabuki, N., and Kitada, K. (1999) Amino acid residues in the ω-minus region participate in cellular localization of yeast glycosylphosphatidylinositol-attached proteins. *J. Bacteriol.* **181,** 3886–3889
64. Caro, L. H., Tettelin, H., Vossen, J. H., Ram, A. F., van den Ende, H., and Klis, F. M. (1997) *In silico* identification of glycosyl-phosphatidylinositol-anchored plasma-membrane and cell wall proteins of *Saccharomyces cerevisiae*. *Yeast* **13,** 1477–1489
65. Bailey, U. M., Jamaluddin, M. F., and Schulz, B. L. (2012) Analysis of congenital disorder of glycosylation-Id in a yeast model system shows diverse site-specific under-glycosylation of glycoproteins. *J. Proteome Res.* **11,** 5376–5383
66. Breidenbach, M. A., Palaniappan, K. K., Pitcher, A. A., and Bertozzi, C. R. (2012) Mapping yeast *N*-glycosites with isotopically recoded glycans. *Mol. Cell. Proteomics* 10.1074/mcp.M111.015339
67. Witt, W., Mertsching, A., and König, E. (1984) Secretion of phospholipase B from *Saccharomyces cerevisiae*. *Biochim. Biophys. Acta* **795,** 117–124
68. Witt, W., Schweingruber, M. E., and Mertsching, A. (1984) Phospholipase B from the plasma membrane of *Saccharomyces cerevisiae*. Separation of two forms with different carbohydrate content. *Biochim. Biophys. Acta* **795,** 108–116
69. Ikushiro, H., Hayashi, H., and Kagamiyama, H. (2004) Reactions of serine palmitoyltransferase with serine and molecular mechanisms of the actions of serine derivatives as inhibitors. *Biochemistry* **43,** 1082–1092
70. Dickson, R. C., Nagiec, E. E., Wells, G. B., Nagiec, M. M., and Lester, R. L. (1997) Synthesis of mannose-(inositol-P)2-ceramide, the major sphingolipid in *Saccharomyces cerevisiae*, requires the *IPT1* (YDR072c) gene. *J. Biol. Chem.* **272,** 29620–29625
71. Zanolari, B., Friant, S., Funato, K., Sütterlin, C., Stevenson, B. J., and Riezman, H. (2000) Sphingoid base synthesis requirement for endocytosis in *Saccharomyces cerevisiae*. *EMBO J.* **19,** 2824–2833
72. Zhang, M., Zhang, Y., Giblin, E. M., and Taylor, D. C. (2009) Ectopic expression of *Arabidopsis* phospholipase A genes elucidates role of phospholipase Bs in *S. cerevisiae* cells. *Open Microbiol. J.* **3,** 136–145
73. De Smet, C. H., Cox, R., Brouwers, J. F., and de Kroon, A. I. (2013) Yeast cells accumulate excess endogenous palmitate in phosphatidylcholine by acyl chain remodeling involving the phospholipase B Plb1p. *Biochim. Biophys. Acta* **1831,** 1167–1176
74. Patton-Vogt, J. L., and Henry, S. A. (1998) *GIT1*, a gene encoding a novel transporter for glycerophosphoinositol in *Saccharomyces cerevisiae*. *Genetics* **149,** 1707–1715
75. Bishop, A. C., Ganguly, S., Solis, N. V., Cooley, B. M., Jensen-Seaman, M. I., Filler, S. G., Mitchell, A. P., and Patton-Vogt, J. (2013) Glycerophosphocholine utilization by *Candida albicans*: role of the Git3 transporter in virulence. *J. Biol. Chem.* **288,** 33939–33952
76. Liu, M., Huang, C., Polu, S. R., Schneiter, R., and Chang, A. (2012) Regulation of sphingolipid synthesis through Orm1 and Orm2 in yeast. *J. Cell Sci.* **125,** 2428–2435
77. Kajiwara, K., Muneoka, T., Watanabe, Y., Karashima, T., Kitagaki, H., and Funato, K. (2012) Perturbation of sphingolipid metabolism induces endoplasmic reticulum stress-mediated mitochondrial apoptosis in budding yeast. *Mol. Microbiol.* **86,** 1246–1261